



Analysis of mass movement susceptibility through fuzzy logic in Itupararanga’s EPA (SP)

Mayra Vanessa Lizcano Toledo

Doutoranda em Ciências Ambientais, UNESP, Brasil.
mayra.lizcano@unesp.br

Ana Laura de Paula

Mestranda em Ciências Ambientais, UNESP, Brasil.
al.paula@unesp.br

Arthur Pereira dos Santos

Doutorando em Ciências Ambientais, UNESP, Brasil.
arthur.p.santos@unesp.br

Darllan Collins da Cunha e Silva

Professor Doutor, UNESP, Brasil.
darllan.collins@unesp.br

Renan Angrizani de Oliveira

Professor Doutor, UNISO, Brasil.
renan.oliveira@prof.uniso.br

ABSTRACT

Considering the recurring events of mass movements and the complexity associated with their causality, as well as the severe socio-environmental consequences triggered by them, it is essential to predict the regions susceptible to this phenomenon. In this context, the objective of this study was to develop a method for analyzing susceptibility to mass movements, implemented in the region of Itapararanga’s Environmental Protection Area (EPA), through the creation of a Mamdani-type Fuzzy inference system. Satellite images and other spatial data were used to create the environmental, pedological, and topographic subsystems, which generated a final output used to classify susceptibility into categories of: very high, high, moderate, low, and very low. The results indicate that areas with higher potential flow index and soil saturation showed higher susceptibility. Additionally, the presence of vegetation and soil type were also determining factors. The final susceptibility map highlighted areas in the north/northwest and south/southeast as highly susceptible to these events, while other regions showed moderate susceptibility. This study provides valuable information for the planning and proper management of areas vulnerable to mass movements.

KEY-WORDS: EPA. mass movements. Mamdani. Susceptibility.

1. INTRODUCTION

Mass movements refer to gravitational displacements, where material is transported by the force of gravity at high speeds (PRANCEVIC et al., 2020). The process is related to the continuous infiltration of rainwater in specific regions with steep slopes, which have soils with saturated pores and higher density (ZHANG et al., 2023). The soil triggers plasticity and high density, starting to have less cohesion between particles, as well as the slope stability angle, leading to an abrupt rupture of the soil (ISMLAM et al., 2021).

Among the causes of mass movements, there are natural and anthropogenic factors (SANTOS et al., 2020). Natural factors are triggered by intense rainfall, with high cumulative rainfall indices, and terrain predispositions (soil morphology, topography, slope, vegetation), while anthropogenic causes result from the suppression of vegetation cover and land use and occupation (FONSECA et al., 2014).

Therefore, vegetation cover is essential in mitigating and preventing mass movements, as it increases soil resistance to shear through root cohesion (COMEGNA et al., 2020). During precipitation events, leaves intercept water droplets and decrease infiltration, preventing soil saturation. Additionally, they reduce soil saturation levels by extracting water through root transpiration. However, their presence does not always guarantee stability, as the interaction between vegetation and soil conditions is complex (PELASCINI, 2023).

Deaths, burying of individuals, injuries, and other fatalities are common in cases of mass movements in inhabited areas. Material damages, high-cost maintenance, losses of homes, and other civil constructions also lead to economic losses in the region affected by a disaster. Thus, mass movements are considered environmental and social disasters, as, in addition to environmental damages such as loss of vegetation cover, erosion, and siltation of water bodies, they can result in tragedies for humans and animals (BAZÁN et al., 2023; UN, 2023; VIEIRA et al., 2023).

Regarding mass movements, susceptibility refers to the predisposition or propensity of terrains to develop this phenomenon (SILVA; AMORIM, 2023), and its determination is essential, especially in watershed management, as it informs land use planning and control, as well as urban expansion restriction (COROMINAS et al., 2014).

To assess this phenomenon, physical, statistical, and knowledge-based evaluation methods are often employed. While the first two are considered traditional and costly, the latter, based on the expertise of specialists in the field, stands out for its generalization capacity and can be implemented through artificial intelligence systems (OSNA et al., 2014; NERY; VIEIRA, 2014). Within this scope are Fuzzy Sets, considered a class of objects with continuous degrees of membership, proposed by Zadeh (1965), where approximations and uncertainties are admitted in contrast to the binary systems of classical logic.

Furthermore, the membership of a Fuzzy set does not infer affirmatives or negatives; instead, it proposes that elements be classified into levels of membership in different sets (DENG; DENG, 2021). Thus, the membership value can take any value between the interval of 0 to 1, where 0 indicates total exclusion and 1 indicates total membership. Moreover, membership sets present various association functions, such as Triangular, Trapezoidal, Sigmoidal, Sine, and Gaussian Combination (YAZDANBAKHS; DICK, 2018).

Although the reasoning is approximate, the product of the Fuzzy proposition is exact, and there are different methods for obtaining precise classical values, a process named defuzzification. Commonly employed methods in this stage include the maximum criterion (MAX), the mean of maximums (MOM), and the center of area method (CDA) (GREENFIELD, 2018; PRAHARAJ; MOHAN, 2021; TAIRIDIS et al., 2016).

According to Greenfield and Chiclana (2013), a Fuzzy inference system has several steps, with the first being the fuzzification of numerical variables, converting the data into fuzzy sets to capture uncertainty. Next, linguistic variables and their values are identified based on specialized knowledge and data analysis. Subsequently, a set of if-then rules is developed to describe the relationships between input and output variables. The partial results of the rules are aggregated to generate the final output of the Fuzzy system. Finally, the fuzzy output is defuzzified to convert it into precise values, allowing for a concise interpretation of the results.

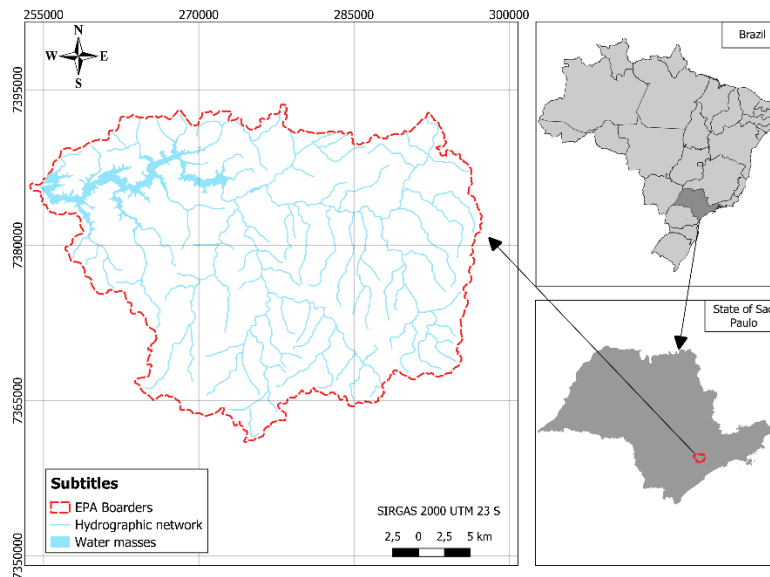
Given that Mamdani-type Fuzzy inference systems are commonly applied in mapping susceptibility to gravitational mass movements when integrated with Geographic Information Systems (GIS) (SOARES et al., 2022), the present study aims to develop a method for analyzing susceptibility to mass movements in an Environmental Protection Area (APA). This involves incorporating topographic, environmental, and pedological variables to develop a fuzzy inference system model that allows for the identification of areas susceptible to mass movements.

2. METHODOLOGY

2.1. Study Field

The object of study is the Conservation Unit (CU) designated as Itupararanga's Environmental Protection Area (EPA) (Figure 1), established by State Law No. 10,100, dated December 1, 1998, and amended by State Law No. 11,579, dated December 2, 2003. It covers an approximate territorial extension of 936.51 km² and is located between the municipalities of Ibiúna, São Roque, Mairinque, Alumínio, Vargem Grande Paulista, Cotia, Votorantim, and Piedade, all in the state of São Paulo (SP) (FUNDAÇÃO FLORESTAL; SMA; SÃO PAULO, 2007).

Figure 1 – Location Map



Source: The authors, 2024.

2.2. Data collection and processing

Initially, it is emphasized that the methodology adopted in this article was based on the study conducted by Vieira et al. (2023), which employed the same input and output variables. However, in this context, three new subsystems were adjusted to enhance the accuracy of the analyzed data.

For the development of the work proposal, seven input variables were established, corresponding to altitude, slope, curvature, topographic wetness index (TWI), stream power index (SPI), soil pedology, and normalized difference vegetation index (NDVI).

The information used for the project development was acquired from the databases of government entities such as the National Institute for Space Research (INPE in Portuguese) and the Brazilian Agricultural Research Corporation (Embrapa in Portuguese). From these sources, the corresponding data for the digital elevation model (DEM) were obtained for calculating variables such as slope, curvature, topographic wetness index (TWI) (Equation 1), and stream power index (SPI) (Equation 2), as well as soil vulnerability, which is obtained from the pedology of the area.

$$TWI = \frac{\alpha}{\tan \beta + C} \quad (1)$$

Where:

α : flow accumulation

β : slope

C: 0.001

$$SPI = \ln(\alpha + 0.001) * \left(\left(\frac{\beta}{100} \right) + 0.001 \right) \quad (2)$$

It's important to add that in the case of NDVI, it was calculated from bands 4 and 5, according to Equation (3), which correspond to the red and near-infrared of the LANDSAT 8-OLI satellite image, acquired from the United States Geological Survey (USGS) website.

$$NDVI = \frac{NIR - RED}{NIR + RED} \quad (3)$$

Where:
 NIR: Infrared
 RED: Red

2.3. Development of the Fuzzy System

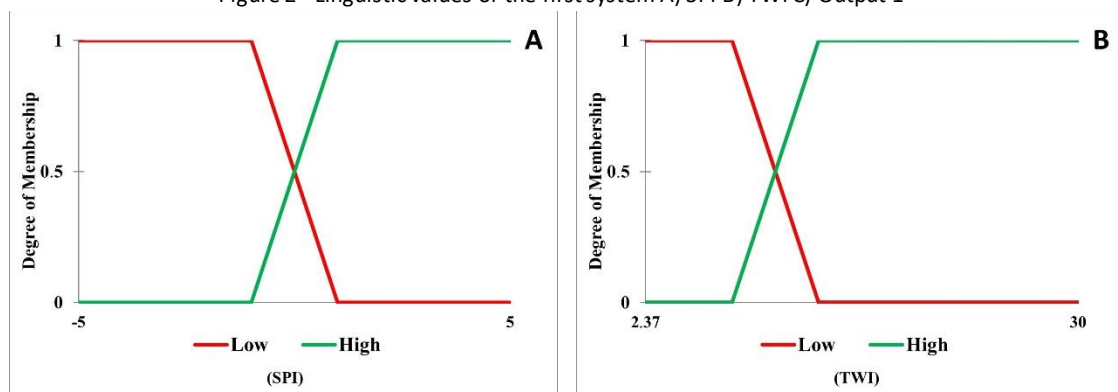
The system was developed so that it can be applied to any field of study, establishing the minimum and maximum possible values for each variable.

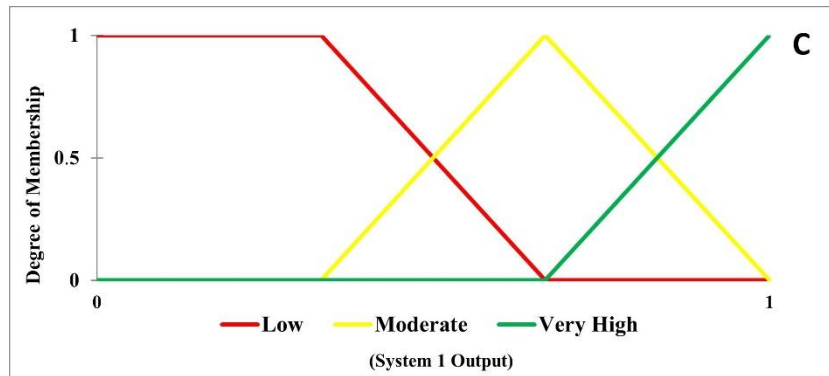
2.3.1. Fuzzification

From the data acquisition and processing, intervals were established for each variable with the assistance of specialized literature, which approaches the classification of the studied variables. Then, linguistic variables and their membership functions were defined for each input based on these identified ranges.

Regarding system 1, the variables identified were the data corresponding to TWI and SPI. For system 2, the input variables are altitude, slope, curvature, and soil pedology, also considered as vulnerability. In the final system, the variables NDVI, the output of system 1, and the output of system 2 were included.

Figure 2 - Linguistic values of the first system A) SPI B) TWI C) Output 1



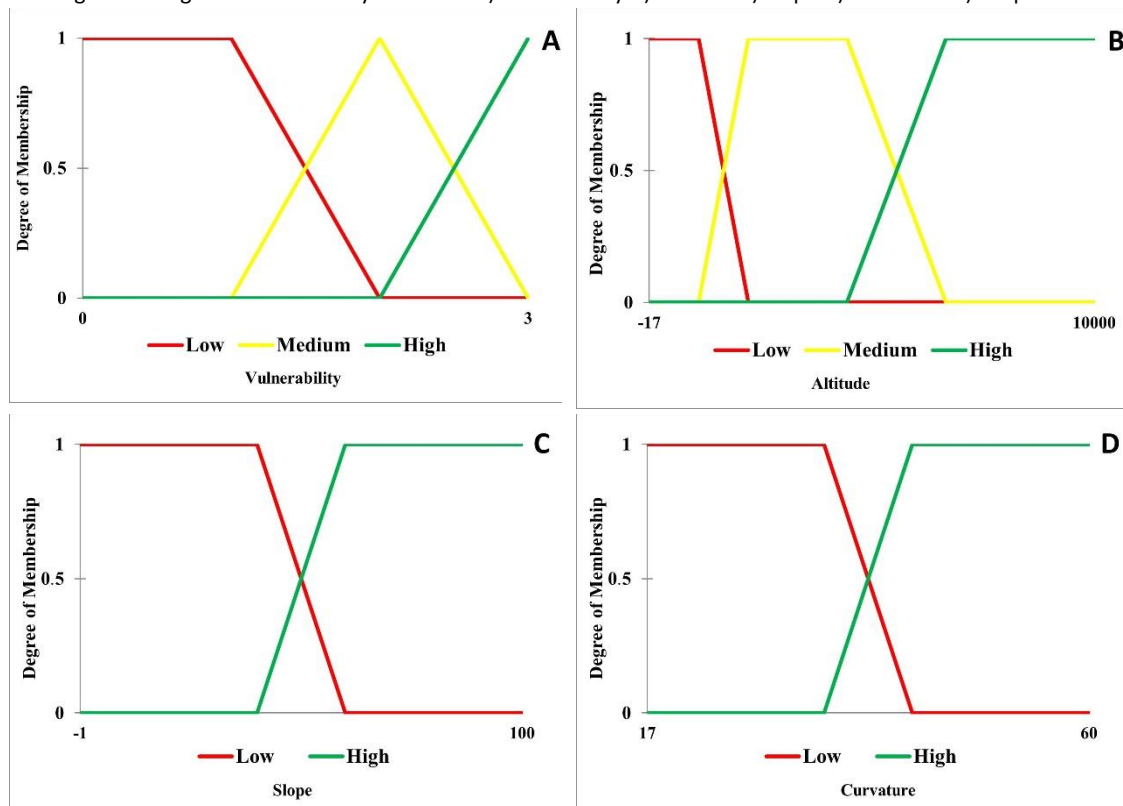


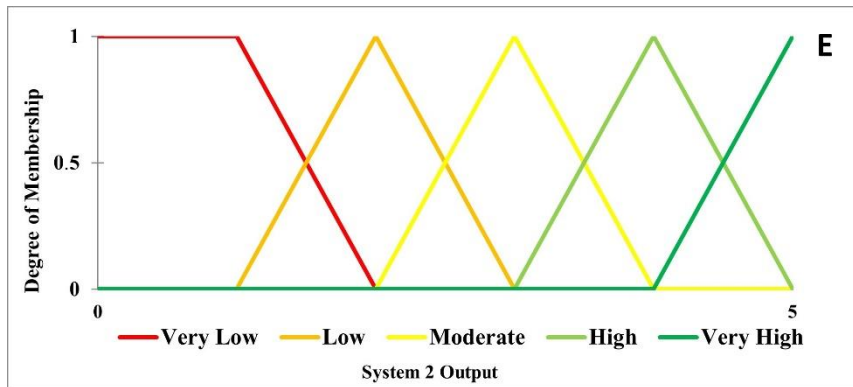
Source: The Authors, 2024.

Regarding the linguistic variables, the input ones were divided into two intervals (Low and High), as shown in Figure 2A and 2B. However, the output variables were established in three, defined as high, moderate, and low, as depicted in Figure 2C.

For system 2, as visualized in Figure 3, for Altitude (Figure 3A) and Soil Pedology (vulnerability) (Figure 3B), low, medium, and high were established. As for Slope (Figure 3C) and Curvature (Figure 3D), two intervals of high and low were defined. Finally, for the system output (Figure 3E), five output classes were generated: very high, high, moderate, low, and very low.

Figure 3 - Linguistic values for system two: A) Vulnerability B) Altitude C) Slope D) Curvature E) Output 2

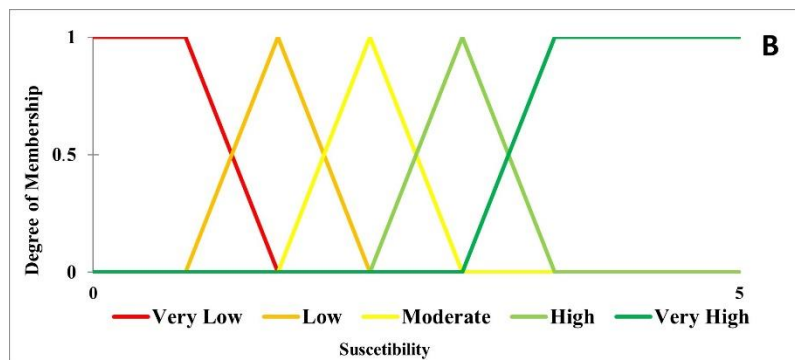
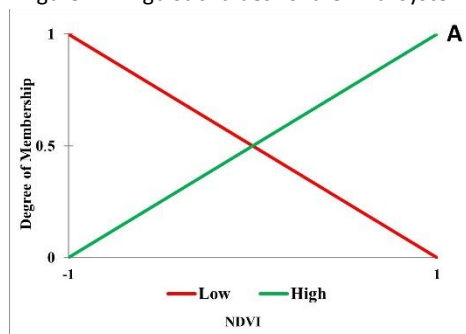




Source: The Authors, 2024.

Finally, the final system, as visualized in Figure 4, is composed of the variables NDVI (Figure 4A), output of system 1 (Figure 2C), and output of system 2 (Figure 3E), with intervals of low and high established for NDVI and five output classes generated for the susceptibility of the study area (Figure 4B).

Figure 4 –Linguistic values for the final system



Source: The Authors, 2024.

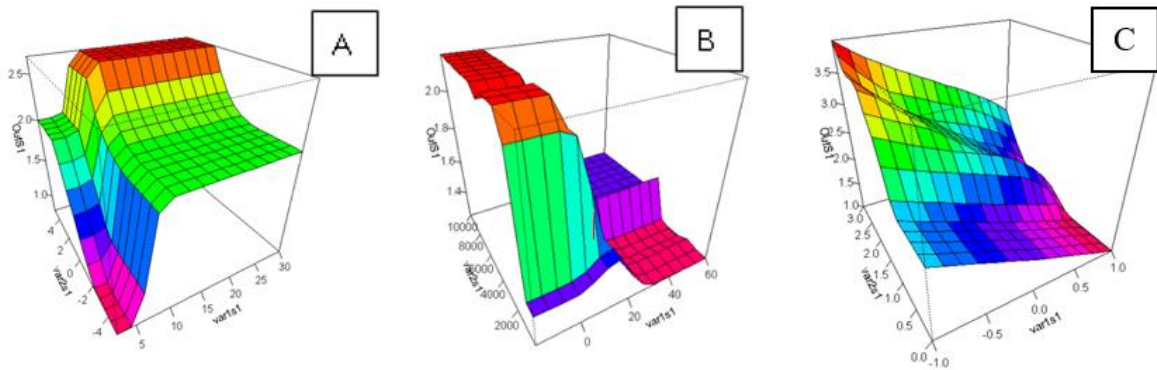
2.3.2. Knowledge base

The developed system is of the Mamdani type, which rules are based on the If A Then B system, where the total number of rules was determined by the quantity of classes for each variable (SILVA et al., 2021). Furthermore, a visualization surface of the behavior of each system was created, aligned with the input variables.

In the knowledge bases depicted in Figure 5, it is possible to observe the surface generated for systems 1, 2, and 3, represented by Figures 5A, B, and C, respectively.

To clarify understanding, rules were established for each system, also respectively arranged.

Figure 5 – Knowledge base: surface (A) System 1 (B) System 2 (C) System 3



Source: The Authors, 2024.

From Table 1, it's possible to identify that 4 rules were generated for the Surface of System 1. Meanwhile, in System 2, due to having the highest number of input variables, the largest number of rules was established, totaling 36, which were defined based on the literature (Table 2). Finally, for the last system, 18 rules were established with 5 output classes (Table 3).

Table 1 – Rules of System 1.

TWI	SPI	Result
Low	Low	Low
Low	High	Moderate
High	Low	Moderate
High	High	High

Source: The Authors, 2024.

Table 2 – Rules of System 2

Curvature	Altitude	Slope	Vulnerability	Result
Low	Low	Low	Low	Low
Low	Low	Low	Moderate	Average
Low	Low	Low	High	High
Low	Low	High	Low	High
Low	Low	High	Moderate	High
Low	Low	High	High	High
High	Low	Low	Low	Very Low
High	Low	Low	Moderate	Very Low
High	Low	Low	High	Low
High	Low	High	Low	Low
High	Low	High	Moderate	Average
High	Low	High	High	High
Low	Moderate	Low	Low	Average
Low	Moderate	Low	Moderate	High
Low	Moderate	Low	High	High
Low	Moderate	High	Low	High
Low	Moderate	High	Moderate	High

Low	Moderate	High	High	Very High
High	Moderate	Low	Low	Very Low
High	Moderate	Low	Moderate	Low
High	Moderate	Low	High	Average
High	Moderate	High	Low	Average
High	Moderate	High	Moderate	High
High	Moderate	High	High	High
Low	High	Low	Low	High
Low	High	Low	Moderate	High
Low	High	Low	High	High
Low	High	High	Low	High
Low	High	High	Moderate	Very High
Low	High	High	High	Very High
High	High	Low	Low	Low
High	High	Low	Moderate	Average
High	High	Low	High	High
High	High	High	Low	High
High	High	High	Moderate	High
High	High	High	High	High

Source: The Authors, 2024.

Table 3 – Rules of System 3

NDVI	Índices	Topografia	Resultado
Low	Low	Low	Low
Low	Low	Moderate	Moderate
Low	Low	High	High
Low	Moderate	Low	Moderate
Low	Moderate	Moderate	High
Low	Moderate	High	Very High
Low	High	Low	High
Low	High	Moderate	Very High
Low	High	High	Very High
High	Low	Low	Very Low
High	Low	Moderate	Very Low
High	Low	High	Low
High	Moderate	Low	Very Low
High	Moderate	Moderate	Low
High	Moderate	High	Moderate
High	High	Low	Low
High	High	Moderate	Moderate
High	High	High	High

Source: The Authors, 2024.

Note: The use of colors in the guidelines of the systems is a way to describe the influence of variables on mass movements. Red represents a significant contribution to the occurrence of these movements, while green indicates a lower risk associated with them.

2.3.3. Defuzzification

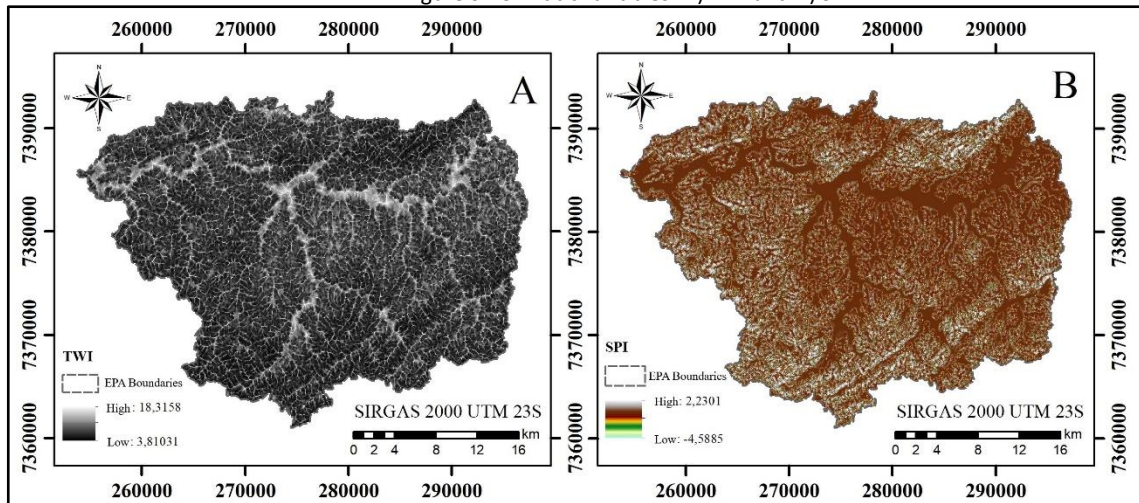
The centroid defuzzification method was chosen, which is based on summing the centers to calculate a crisp value, used to create a landslide susceptibility map in ArcGIS.

3. RESULTS AND DISCUSSION

For the 3 systems, 7 variables were used, allocated within each system's categories. Four rules were obtained for the climate variable system, 36 rules for the topographic variable system, and to the final system, the outputs of the previous systems were added to the environmental variable, resulting in a total of 18 rules.

In Figure 6, the values of the climatic variables used in the first system are visualized. In the case of TWI (Figure 6A), the values within Itupararanga’s EPA range from 3.81 to 18.31, which, as stated by Milevski et al. (2009), the higher the potential flow index, the higher the probability of mass movement occurrence. Due to the soil saturation level, based on the values identified for the study area, the area is classified as moderately susceptible (SINGH et al., 2021).

Figure 6 - Climatic variables: A) TWI and B) SPI

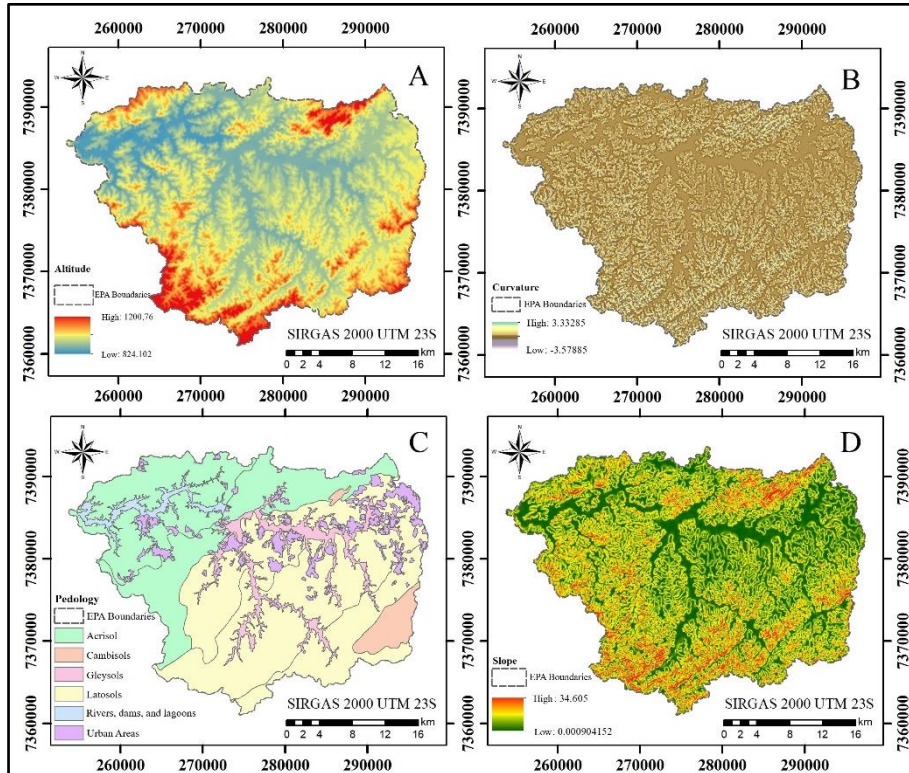


Source: The Authors, 2024.

The SPI (Figure 6B) is evaluated as an important measure for identifying susceptibility to mass movements, considering the spatial distribution of moisture in the terrain, taking into account factors such as topography and vegetation (CHEN; CHANG, 2016). According to Oh and Pradhan (2011), through topographic moisture, it is possible to identify areas where water tends to accumulate. Areas with high SPI are more susceptible to mass movements because soil saturation reduces resistance and cohesion, promoting instability and mass movements. The values ranged from -4.588 to 2.23, thus, the areas are classified as moderately and strongly susceptible.

Figure 7 highlights the topographic variables represented by altitude (Figure 7A), curvature (Figure 7B), pedology (Figure 7C), and slope (Figure 7D), used as input in the second system.

Figure 7 - Topographic variables: A) Altitude, B) Curvature, C) Pedology, and D) Slope



Source: The Authors, 2024.

According to Gholami et al. (2019), higher altitude areas indicate lower temperatures and higher precipitation, which increases soil saturation. When associated with mountainous regions, these areas typically have steeper terrains, making them more susceptible to mass movements. Altitude influences soil characteristics, resulting in high concentrations of clay and/or undecomposed rock materials, defined by greater fragility and lower cohesion. Additionally, in Itupararanga's Environmental Protection Area (EPA), an altimetric variation between 824.10 and 1200.76 m was observed.

Regarding curvature, Altin and Gökkaya (2018) state that convex curvatures reduce the amount of water that can infiltrate the soil, decreasing its saturation and thus reducing the probability of mass movements. However, concave and flat curvatures tend to increase the amount of water that can infiltrate the soil, leading to a higher susceptibility to mass movement. Therefore, based on the values obtained for curvature in the study area, this variable is categorized as moderately susceptible.

According to Viera et al. (2023), pedology is determinant for mass movements, as soils with a higher sand content tend to be more susceptible to such events compared to clayey soils. The Acrisol soil class is considered intermediate, with shallower depth, less stability, and impermeability. On the other hand, Latosols have greater depth and porosity, leading to more stability. Cambisols and Gleysols are recognized as younger soils and exhibit greater vulnerability to mass movements (SILVEIRA et al., 2014; IBGE, 2019).

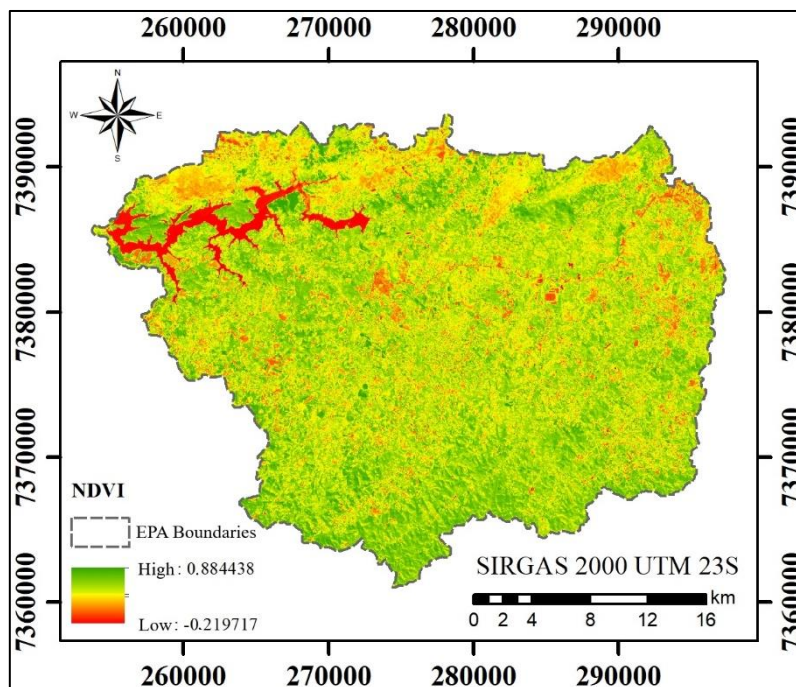
In the study area, mainly Acrisol soils are found, covering an area of 211,373.49 ha, representing 59.73% of the study area, followed by Latosols with 95,225.96 ha (26.91%), Cambisols with 41,032.90 ha (11.60%), and Gleysols with 6,226.97 ha (1.76%).

Consequently, the terrain slope can play a significant role in the susceptibility of an area to mass movements. Steeper terrains have a higher potential for such events because they are more susceptible to erosion when devoid of vegetation, where mass movements can occur more rapidly and with greater magnitude (IBGE, 2019; SIMONETTI et al., 2022).

Regarding the environmental variable represented by NDVI (Figure 8), it is known that values close to 1 indicate significant vegetation vigor, while values close to 0 suggest sparser vegetation, and negative values indicate the presence of water bodies or urban areas (LI; DUAN, 2024).

In the study area, NDVI values ranged from approximately -0.22 to 0.88, with a predominance of intermediate values, as highlighted on the map by the representation of the color yellow, indicating a moderate amount of vegetation, subject to fluctuations according to environmental and seasonal conditions (NIRAJ et al., 2023; RIZZO et al., 2023).

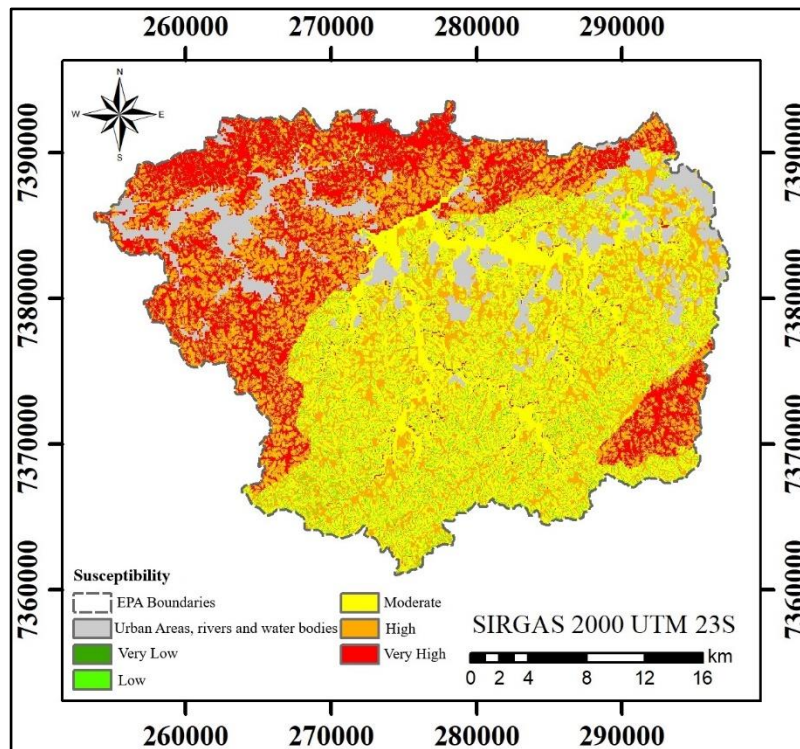
Figure 8 - Environmental variable: NDVI



Source: The Authors, 2024.

Regarding the final map of susceptibility to mass movements (Figure 9), areas identified as having very high susceptibility are mainly located in the northern/northwestern and southern/southeastern portions of the study area, with a high prevalence of this classification.

Figure 9 - Susceptibility to mass movements



Source: The Authors, 2024.

Predominantly, the rest of the area exhibits moderate susceptibility, with significant evidence of high susceptibility throughout the entire extent of the EPA. The gray portions were excluded from the assessment as they are categorized as urban areas, rivers, and water bodies.

It is observed that in areas where there is a combination of low to moderate vegetation presence, along with the predominant Acrisols in the region, characterized as vulnerable, this is where areas with very high susceptibility to mass movements are concentrated.

Furthermore, variables such as TWI and SPI indicate a higher probability of mass movements in areas with higher flow potential and soil saturation indices. Topographic characteristics, such as altitude, curvature, and slope, also contributed, showing that areas with higher altitude and concave curvature tend to be more susceptible.

4. CONCLUSION

The study demonstrated the effectiveness of using Fuzzy inference systems in analyzing susceptibility to mass movements in Itapararanga’s EPA, as well as integrating topographic, environmental, and pedological variables. Thus, making it possible to identify areas at high risk of mass movements and providing significant information regarding the analysis of vulnerable areas.

The results indicated that the study area is predominantly vulnerable to mass movements, with high susceptibility in the northern/northwestern and southern/southeastern regions. Topographic variables such as altitude, curvature, and slope played a crucial role in identifying these high-risk areas. Therefore, there is a need to implement mitigation measures

to enable proper planning and management of vulnerable areas, thus promoting environmental and population safety in the region.

5. REFERENCES

- ALTIN, T. B.; GÖKKAYA, E. Assessment of landslide-triggering factors and occurrence using morphometric parameters in Geyraz Basin, Tokat, Northern Turkey. **Environment Earth Sciences**, 2018. doi: 10.1007/s12665-018-7315-8.
- BAZÁN, F.; CRUZ, A. M.; AZEVEDO, G.; QUEIROZ, P. C. Susceptibilidade de taludes a deslizamentos de terra no município de São Luís/MA. **REVISTA FOCO**, v. 16, n. 6, p. e2123-e2123, 2023 doi: 10.54751/revistafoco.v16n6-018.
- CHEN, CY.; CHANG, JM. Landslide dam formation susceptibility analysis based on geomorphic features. **Landslides**, v. 1, p. 1019 – 1033. 2016. doi: 10.1007/s10346-015-0671-5.
- COMEGNA, L.; PICARELLI, L.; URCIUOLI, G. Efeitos dos movimentos de encostas na estrutura do solo e na resposta hidrológica. **Engenharia Geotécnica e Geológica**, v. 38, 2020. doi: 10.1007/s10706-020-01341-2.
- COROMINAS, J.; WESTEN, C.; FRATTINI, P.; CASCINI, L.; MALET, J.; FOTOPOULOU, S.; CATANI, F.; EECKHAUT, V.; MAVROULI, O.; AGLIARDI, F.; PITILAKIS, K.; WINTER, M.; PASTOR, M.; FERLISI, S.; TOFANI, V.; HERVÁS, J.; SMITH, J. Recommendations for the quantitative analysis of landslide risk. **Bulletin of Engineering Geology and the Environment**, v. 73, p. 209 – 263. 2014. doi: 10.1007/s10064-013-0538-8.
- DENG, J.; DENG, Y. Information Volume of Fuzzy Membership Function. **International Journal of Computers Communication & Control**, v. 16, 2021. doi: 10.15837/IJCCC.2021.1.4106.
- FONSECA, L. M.; LANI, J.; FILHO, E.; SANTOS, G.; FERREIRA, W.; SANTOS, A. Variability in soil physical properties in landslide-prone areas. **Acta Scientiarum. Agronomy**, v. 39, n. 1, 2017. doi: 10.4025/actasciagron.v39i1.30561.
- FUNDAÇÃO FLORESTAL; SMA - SECRETARIA DO MEIO AMBIENTE, SÃO PAULO - GOVERNO DE SÃO PAULO **Plano de manejo da área de proteção ambiental (APA) Itupararanga**. 2007. Disponível em: fflorestal.sp.gov.br/planos-de-manejo/planos-de-manejo-planos-concluidos/plano-de-manejo-apa-itupararanga.
- GHOLAMI, M.; GHACHKANLU, KHOSRAVI, K.; PIRASTEH, S. Landslide prediction capability by comparison of frequency ratio, fuzzy gamma and landslide index method. **Journal of Earth System Science**, v. 128, n. 42, 2019. doi: 10.1007/s12040-018-1047-8.
- GREENFIELD, S. Geometric Defuzzification revisited. **Information Sciences**, v. 466, 2018. doi: 10.1016/j.ins.2018.07.019.
- GREENFIELD, S.; CHICLANA, F. Defuzzification of the discretised generalised type-2 fuzzy set: Experimental evaluation. **Information Sciences**, v. 244, 2013. doi: 10.1016/j.ins.2013.04.032.
- IBGE. Macrocaracterização dos Recursos Naturais do Brasil: Suscetibilidade a deslizamentos do Brasil prim eira aproximação, 2019. Disponível em: biblioteca.ibge.gov.br/visualizacao/livros/liv101684.pdf. Acesso em: 05 mar. 2024.
- ISLAM, S.; BEGUM, A.; HASAN, M. Slope stability analysis of the Rangamati District using geotechnical and geochemical parameters. **Natural Hazards**, v.108, p. 1659 – 1686. 2021. doi: 10.1007/s11069-021-04750-5.
- LI, Y.; DUAN, W.; Decoding vegetation's role in landslide susceptibility mapping: An integrated review of techniques and future directions. **Biogeotechnics**, v. 2, 2024. doi: 10.1016/j.bgtech.2023.100056.
- MILEVSKI, I.; MARKOSKI, B.; GORIN, S.; JOVANOVSKI, M. **Application of remote sensing and GIS in detection of potential landslide areas**. Proceedings of the international symposium geography and sustainable development, Ohrid. p. 453-463. 2009.
- NERY, T. D.; VIEIRA, B. C. Susceptibility to shallow landslides in a drainage basin in the Serra do Mar, São Paulo, Brazil, predicted using the SINMAP mathematical model. **Bulletin of Engineering Geology and the Environment**, 2014. doi: 10.1007/s10064-014-0622-8.
- NIRAJ, K. C.; SINGH, A.; SHUKLA, D. P. Efeito do Índice de Vegetação por Diferença Normalizada (NDVI) em Modelos Estatísticos Bivariados e Multivariados Habilitados para GIS para Mapeamento de Suscetibilidade a Deslizamentos. **Journal of the Indian Society of Remote Sensing**, v. 51, 2023. doi: 10.1007/s12524-023-01738-5.

OH, H.; PRADHAN, B. Application of a neuro-fuzzy model to landslide-susceptibility mapping for shallow landslides in a tropical hilly area. **Computers & Geosciences**, v. 37, 2011.

ONU. **Retrocessos evidentes nos esforços globais para conter os desastres naturais**. 2023. Disponível em: news.un.org/pt/story/2023/05/1814597#:~:text=Entre%20os%20retrocessos%20est%C3%A1%20o,ano%20entre%202015%20e%202021. Acesso em: 10 mar. 2024.

OSNA, T.; SEZER, E. A.; AKGUN, A. GeoFIS: an integrated tool for the assessment of landslide susceptibility. **Computers & Geosciences**, v. 66, 2014.

PELASCINI, L. **Impacts of typhoons and hydraulic conditions on hillslopes stability**. 2023. Tese de Doutorado. Université de Rennes.

PRAHARAJ, M.; BOSUKONDA, M.; Modeling and Analysis of Mamdani Two-Term Controllers Using Non-Uniformly Distributed Multiple Fuzzy Sets and CoA/CoG Defuzzification. **IETE Technical Review**, v. 39, n. 4, 2021. doi: 10.1080/02564602.2021.1933628.

PRANCEVIC, J. LAMB, M.; MCARDELL, B.; RICKLI, C.; KIRCHNER, J. Decreasing Landslide Erosion on Steeper Slopes in Soil-Mantled Landscapes. **Geophysical Research Letters**, v. 47, 2020. doi: 10.1029/2020GL087505.

RIZZO, F. A.; SACRAMENTO, B. H.; TONELLO, P. S.; SILVA, D. C. C. Proposta metodológica de identificação de áreas prioritárias para recuperação da bacia hidrográfica do córrego Pequiá (MA). **REVISTA TECNOLOGIA E SOCIEDADE (ONLINE)**, v. 19, p. 33-54, 2023. DOI: <https://doi.org/10.20502/rbg.v23i1.2037>

SILVA, D. C. C.; OLIVEIRA, R. A.; SIMONETTI, V. C.; ANDRADE, E. L.; SOUSA, J. A. P.; SALES, J. C. A.; LOURENÇO, R. W. Application of fuzzy systems to support the development of a socioenvironmental sustainability index applied to river basins. **International Journal of River Basin Management**, p. 1-13, 2021. DOI: <https://doi.org/10.1080/15715124.2021.1938093>

SILVA G.; AMORIM, R. R. **Suscetibilidade e vulnerabilidade: um impasse conceitual que dificulta a responsabilização pelo desastre**. anais do evento em comemoração aos 20 anos do programa de pós-graduação em geografia (ig-unicamp), v. 1, n. 1, p. 50-65, 2023.

SILVEIRA, H.; VETTORAZZI, C.; VALENTE, R. Avaliação multicriterial no mapeamento da suscetibilidade de deslizamentos de terra. **Revista Árvore, viçosa-MG**, v.38, n.6, p.973-982. 2014.

SIMONETTI, V. C.; SILVA, D. C. C.; ROSA, A. H. Correlação espacial compartimentada dos padrões de drenagem com características morfológicas da bacia hidrográfica do rio Pirajibu-Mirim. **Revista Brasileira de Geomorfologia**, v. 23, p. 1134-1154, 2022. DOI: <https://doi.org/10.3895/rts.v19n57.15589>

SINGH, P.; SHARMA, A.; SUR, U.; RAI, P. K. Comparative landslide susceptibility assessment using statistical information value and index of entropy model in Bhanupali-Beri region, Himachal Pradesh, India. **Environment, Development and Sustainability**, v. 23, p. 5233 – 5225. 2021. doi:10.1007/s10668-020-00811-0.

SOARES, Jr. A. V.; BARRADAS, T. F.; FRANCHI, J. F. Dados geológicos e de sensoriamento remoto aplicados ao mapeamento da suscetibilidade a movimentos de massa: estudo de caso em Mairiporã, Estado de São Paulo – Brasil. **Boletim Paranaense de Geociências**, v. 80, n. 2, p. 166 – 187. 2022.

TAIRIDIS, G.; FOUTSITZI, G.; KOUTSIANITIS, P.; STAVROULAKIS, G. Fine tuning of a fuzzy controller for vibration suppression of smart plates using genetic algorithms. **Advances in Engineering Software**. v. 101, p. 123 – 135, 2016. doi: 10.1016/j.advengsoft.2016.01.019.

VIEIRA, A.; PESSOA, F.; ATAIDE, L. Avaliação do mapeamento de suscetibilidade de deslizamento de terra em uma Bacia Amazônica via Lógica Fuzzy. **Revista Geoaraguaia**, v. 13, n. 1, p. 54-73, 2023.

ZADEH, L. A. Fuzzy sets. **Information and Control**. v. 8, n. 3 p. 338 – 353, 1965 doi: 10.1016/S0019-9958(65)90241-X.

ZHANG, Z.; ZENG, R.; MENG, X.; ZHAO, S.; WANG, S.; MA, J.; WANG, HONG. Effects of changes in soil Properties caused by progressive infiltration of Rainwater on rainfall-induced-landslides. **Catena**, v. 233, 2023 doi: 10.1016/j.catena.2023.107475.